A Crystallographic and Spectroscopic Study of the Complex between d(CGCGAATTCGCG)$_2$ and 2,5-Bis(4-guanylphenyl)furan, an Analogue of Berenil. Structural Origins of Enhanced DNA-Binding Affinity†

Charles A. Laughton,‡ Farial Tanious,§ Christine M. Nunn,‡ David W. Boykin,§ W. David Wilson,§ and Stephen Neidle*,‡

The CRC Biomolecular Structure Unit, The Institute of Cancer Research, Sutton, Surrey SM2 5NG, U.K., and Department of Chemistry, Georgia State University, Atlanta, Georgia 30303

Received September 11, 1995; Revised Manuscript Received February 26, 1996⊗

ABSTRACT: 2,5-Bis(4-guanylphenyl)furan ("furamidine") is a dicationic minor groove binding drug that has been shown to be more effective than pentamidine against the *Pneumocystis carinii* pathogen in an immunosuppressed rat model. It has a close structural similarity to the antitrypanosomal drug berenil, differing only in the replacement of the central triazene unit with a furan moiety. We have determined the crystal structure of the complex between furamidine and the DNA dodecamer d(CGCGAATTCGCG)$_2$ and compared it to the corresponding berenil complex. We have also compared the interaction of these two ligands with the same DNA sequence by UV−visible, fluoresence, and CD spectroscopy. Furamidine shows tighter binding to this sequence ($K_{eq} = 6.7 \times 10^6$) than berenil ($K_{eq} = 6.6 \times 10^5$). The crystal structure reveals that, unlike berenil, furamidine makes direct hydrogen bond interactions with this DNA sequence through both amidinium groups to O2 atoms of thymine bases and is more isohelical with the minor groove. Molecular mechanics calculations support the hypothesis that these differences result in the improved interaction energy between the ligand and the DNA.

As the number of complexes between DNA and minor groove binding ligands that have been solved by X-ray crystallography (Kopka et al., 1985; Coll et al., 1989; Brown et al., 1990, 1992; Gao et al., 1993; Tabernero et al., 1993; Nunn et al., 1994; Goodsell et al., 1995) and NMR (Klevit et al., 1986; Patel & Shapiro, 1986; Lee et al., 1988; Pelton & Wemmer, 1989; Kumar et al., 1990, 1991; Parkinson et al., 1990; Searle & Embrey, 1990; Fede et al., 1991; Singh et al., 1992; Jenkins et al., 1993; Sriram et al., 1994) increases, it is becoming possible to identify structural considerations that govern observed patterns of sequence selectivity and affinity. Some of these factors are relatively self-evident, such as the requirement for overall shape complementarity between the ligand and the minor groove surface (isohelicity) (Goodsell & Dickerson, 1986) and for complementarity in hydrogen-bonding and electrostatic characteristics (Zakrzewska et al., 1987) between the ligand and a DNA binding site. However, others are more subtle, such as the influence of sequence-dependent DNA flexibility (Ulyanov & Zhurkin, 1984; Laughton et al., 1990; Zhurkin et al., 1991), sequence-dependent minor groove width, and the role of water molecules (Brown et al., 1990).

2,5-Bis(4-guanylphenyl)furan ("furamidine", **1**) is a dicationic minor groove binding drug that has been shown to be more effective than pentamidine against the AIDS-associated pathogen *Pneumocystis carinii* in an immunosuppressed rat model (Boykin et al., 1995) . Structure-activity studies have shown that activity against *P. carinii* correlates with strength of binding to AT sequences in DNA, possibly because of the existence of extended AT tracts in the genome of this pathogen. Furamidine has a close structural similarity (Figure 1) to berenil (**2**), differing only in the replacement of the central triazene linker by a furan ring. The structures of berenil complexes with the sequences d(CGCGAATTCGCG)$_2$ and d(CGCAAATTTGCG)$_2$ have previously been solved by X-ray crystallography in this laboratory (Brown et al., 1990, 1992), and we have recently published a preliminary account of the medicinal chemistry of **1** (Boykin et al., 1995). Here we describe in detail the crystal structure of the complex between **1** and d(CGCGAATTCGCG)$_2$ and compare it to the related berenil complex. In addition, we describe biophysical studies on the interaction of the two ligands with the same DNA sequence and show how structural data can help to explain differences between the ligands revealed by these experiments.

EXPERIMENTAL PROCEDURES

Synthesis and Crystallization. The DNA dodecamer d(CGCGAATTCGCG)$_2$ was purchased from the Oswel DNA Service (University of Southampton, U.K.) and annealed before use. 2,5-Bis(4-guanylphenyl)furan hyrochloride (**1**) was synthesized as described previously (Das & Boykin, 1977) .

Colorless crystals of the complex were grown from sitting drops at 286 K. The crystal used for data collection was obtained from a drop containing 4 μL of 40% w/w 2-methylpentane-2,4-diol (MPD), 2.5 μL of 5 mM **1**, 2 μL of 200 mM $MgCl_2$, 1.5 μL of 2.4 mM spermine, and 4 μL of 3 mM dodecamer equilibrated against a reservoir of 4 mL of 40% MPD for 2 weeks. All solutions were prepared using 30 mM sodium cacodylate buffer at pH 7.0.

† This work was supported by Grant SP1384 from the Cancer Research Campaign of Great Britain (to S.N.) and by NIH Grant AI-33363 (to D.W.B. and W.D.W.).

* Corresponding author. Tel: (44) 181 643 8901 Ext 4251. Fax: (44) 181 643 1675. Email: steve@iris5.icr.ac.uk.

‡ The Institute of Cancer Research.

§ Georgia State University.

⊗ Abstract published in *Advance ACS Abstracts,* April 15, 1996.

S0006-2960(95)02162-3 CCC: $12.00

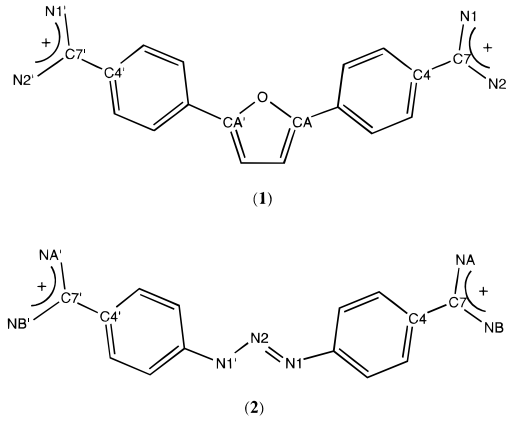

FIGURE 1: Structure and partial numbering scheme for furamidine (**1**) and berenil (**2**).

Data Collection. A crystal (approximate dimensions 0.5 × 0.3 × 0.15 mm) was mounted in a 0.5 mm Lindemann glass capillary with a small amount of the mother liquor. Intensity data were collected at 287 K using a Siemens-Xentronics multiwire area detector mounted on a rotating anode X-ray generator (40 kV, 70 mA) equipped with a graphite monochromator. A crystal-to-detector distance of 10cm and swing angle of 15° were used to obtain data to a maximum resolution of 2.2 Å. With χ set at 45°, data sets were collected using $\phi = 0°$ and $\phi = -60°$. In each case the crystal was rotated through 100° in ω, collecting 180 s frames every 0.2°. No crystal decay was apparent.

Data processing was carried out using XENGEN 1.3. A total of 8693 out of a possible 10 479 reflections were collected to a resolution of 2.2 Å. Merging of the data yielded 3472 unique reflections out of a possible 3895 (89%) with a merging R-value of 8.8%. For the data in the highest resolution range, 2.4−2.2 Å, 74% of the reflections were observed, of which 55% had intensities greater than 2σ.

Structure Refinement. All crystallographic refinement was performed using the program X-PLOR Version 3.1 (Brunger et al., 1987). The unit cell dimensions are $a = 25.28$ Å, $b = 40.69$ Å, and $c = 66.73$ Å, and the space group is $P2_12_12_1$, suggesting a structure isomorphous with the native dodecamer sequence and many related drug complexes. Therefore, for a starting model for the refinement we used the coordinates of the DNA from the γ-oxapentamidine complex solved in this laboratory (Nunn et al., 1994). Rigid-body refinement using data in the range 8.0−3.5Å [871 reflections with $F > 2\sigma(F)$] gave an R factor of 29.2%. Rigid group refinement with the DNA divided into 70 groups (one for each base, sugar and phosphate) and the same resolution range reduced the R factor to 22.9%. Four rounds of positional refinement, extending the resolution range in stages to 2.2Å (2475 reflections with the same σ cutoff), led to an R factor of 26.6%, and a subsequent round of B factor refinement reduced this to 24.6%. At this stage electron density maps, displayed using the graphics package "O" (Jones et al., 1991) revealed a clear volume of density in the DNA minor groove which, though not completely continuous, provided a good fit to an energy-minimized model for furamidine (**1**). Partial charges for furamidine were calculated using MOPAC/ESP (Stewart, 1990) and other force-field parameters not present in the standard X-PLOR database were obtained by interpolation. Positional and B factor refinement led to an R factor of 22.9%. In the course of a further 11 rounds of map generation, assignment of solvent (water) positions, and positional and B factor refinement, 54 waters were added, and the R factor was reduced to 17.8%. Final atomic coordinates and structure factors have been deposited in the Brookhaven Protein Data Bank as entry number 227D.

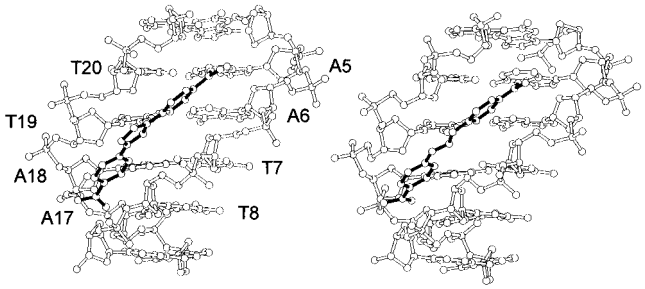

FIGURE 2: Structures of (left) the complex between furamidine and the DNA dodecamer d(CGCGAATTCGCG)$_2$ and (right) the berenil complex (Brown et al., 1990). In both cases only the six central base pairs are shown, and the ligands have been drawn with darkened bonds.

Molecular Modeling. Calculations of the interaction energy between the DNA and drugs in the crystal structures were performed using the AMBER 4.0 suite of programs (Pearlman et al., 1991) and the standard all-atom force field (Weiner et al., 1986). Nonbonded interactions were calculated using a 9 Å cutoff. The crystallographic water molecules were not included in the analysis; instead, the influence of solvent on electrostatic interactions was modeled by using a distance-dependent dielectric constant of 4 (Orozco et al., 1990) . In the same way as for furamidine (**1**), partial charges for berenil were calculated using MOPAC/ESP. As only nonbonded interactions were analyzed, other force-field parameters for the drugs not present in the standard database were given nominal values.

Materials for Biophysical Studies. MES buffer contained 0.01 M MES and 1×10^{-3} M EDTA. Sodium chloride was added to adjust the ionic strength, and the pH was adjusted to 6.2 with NaOH. The oligomer d(CGCGAATTCGCG) (Midland Certified Reagent Co.) was purified by HPLC. The concentrations were determined optically using extinction coefficients per mole of strand at 260 nm determined by the nearest neighbor procedure (Fasman, 1975).

Biophysical Methods. UV−vis scans were obtained with Cary 3 or Cary 4 spectrophotometers as previously described (Wilson et al., 1985) in MES with 0.2 M NaCl added.

CD spectra were obtained on a Jasco J-710 spectrometer interfaced to an IBM-PC computer. The software supplied by Jasco provided instrument control, data acquisition, and manipulation. Solutions of the compounds in MES buffer with 0.1 M NaCl at 25 °C were scanned in 1 cm quartz cuvettes. A solution of the DNA was scanned, the compound was then added, and the sample was rescanned at all desired ratios.

Kinetic measurements were conducted on a Hi-Tech SF-51 stopped-flow spectrometer as previously described (Tanious et al., 1992).

RESULTS

The Structure of the Complex. Furamidine (**1**) was observed to lie in the central region of the minor groove of the B-form d(CGCGAATTCGCG)$_2$ duplex (Figures 2 and 3). Isohelicity between **1** and the minor groove is produced

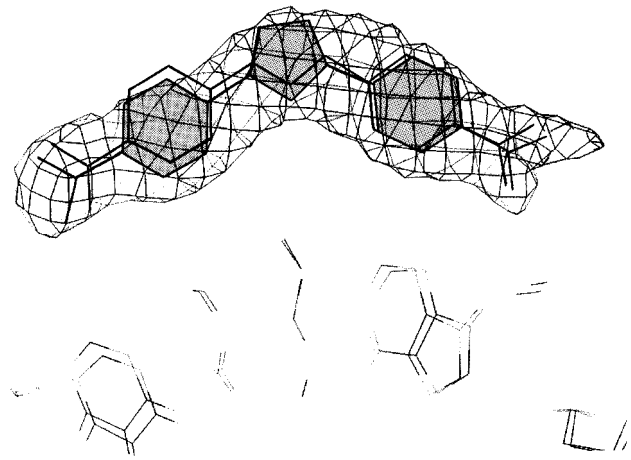

FIGURE 3: A portion of the $F_o - F_c$ omit map, contoured at the 2.5σ level, calculated with the furamidine molecule omitted. The position of the berenil molecule as found in the structure of the berenil−d(CGCGAATTCGCG)$_2$ complex (Brown et al., 1990) has been superimposed onto the density.

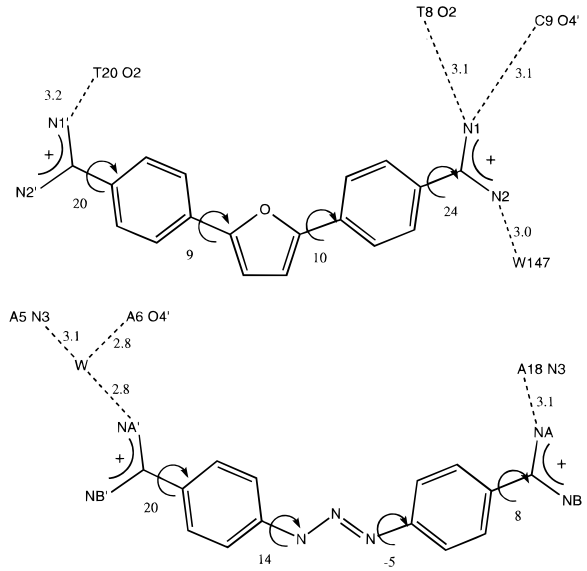

FIGURE 4: Comparison of the hydrogen bonds between the ligand and the DNA and water molecules observed in (top) the present furamidine structure and (bottom) the berenil (2DBE) crystal structure. Ligand torsion angles are also shown.

by rotations about the bonds connecting the (essentially planar) amidinium, phenyl, and furan moieties in **1** (Figure 4). The inner-facing nitrogen of one amidinium group (N1) is hydrogen-bonded to the O2 atom of T8 (3.1 Å), while the inner-facing nitrogen of the other amidinium (N1′) hydrogen-bonds to the O2 of T20 (3.2 Å), four base pairs away. There are close van der Waals contacts between **1** and the DNA (Figure 5), in particular between carbon atoms CB and CB′ of the furan ring and the sugars of T8 and T20, on opposite strands of the DNA. In Figure 5 these produce the two "fingers" in the contact surface that wrap around opposite faces of the furan ring.

The Structure of the DNA. We have compared the structure of the DNA with that observed in the crystal stucture of the corresponding berenil complex (2DBE) (Brown et al., 1990) and with one of the native structures (7BNA) (Holbrook et al., 1985). We identify the bases in the first strand as C1 to G12 and in the second strand as C13 to G24. A comparison of helical parameters (calculated using the program CURVES; Lavery & Sklenar, 1988) for the present structure, 2DBE, and 7BNA shows that the most noticeable differences are in the buckle profile (Figure 6). At base pair G2−C23 the current structure has a buckle closer to the native structure than the berenil complex, but at base pairs G4−C21, A5−T20, and A6−T19 in particular, the buckle profile is rather different from that observed in either the native or berenil complex structures. The maximum difference in this parameter between the present structure and these two others is 5−6°, which is significant in relation to the probable esd for buckle of 2−3°. The possible origin of these differences is discussed below. Comparison of minor groove widths shows that furamidine produces the same increase in the width of the central region of the minor groove as does berenil (Figure 7).

Comparison with the Dodecamer/Berenil Structure. Although the overall structures of the furamidine−dodecamer and berenil−dodecamer complexes are very similar (Figure 2), they differ in detail in two important respects. (1) Furamidine makes two direct hydrogen bond contacts with the DNA, through both its amidinium groups, whereas only one amidinium group in berenil interacts directly with the DNA. (2) The second interaction, at the other end of the berenil ligand, is mediated through a water molecule (Figure 4). This water molecule was clearly visible in the electron density maps of the berenil complex, even at the moderate 2.5 Å resolution of the structure (Brown et al., 1990). No such water molecule has been observed in the present structure. The result is that the furamidine molecule has a four base pair binding site whereas berenil has a three base pair site. Berenil in its complex has been observed to interact with adenines, A5 and A17. Amidinium N1 of furamidine is 4.5 Å distant from atom N3 of adenine A17 (and 3.8 Å distant from atom N3 of adenine A18), while the other amidinium, N1′, is 4.1 Å from N3 of A5. Furamidine therefore does not bind in the same way since these distances (N1···N3A17, N1′···N3A5, and N1···N3A18) are far too long to be considered as hydrogen bonds, even taking into account the likely uncertainties in distances in this structure (±0.1 Å). Examination of the structures suggests that this may be more a reflection of differences in the structure of the ligands rather than being due to changes in the conformation of the DNA. First, furamidine is a slightly longer molecule than berenil; the distance between the C7 and C7′ atoms in furamidine is 12.5 Å, but only 11.9 Å in berenil. The overlay of the two structures on the omit map (Figure 3) shows that the density at both ends is slightly too long for berenil but is better fitted by the furamidine molecule. This size difference is due in part to a difference in the splay angle between the two phenylamidinium groups; the angle between the vectors CA−C4 and CA′−C4′ in the furamidine structure is 125°, whereas that between the corresponding vectors N1−C4′ and N1′−C4′ in the berenil structure is 121°. It may be argued that these differences lie at the limit of what may be considered observable in structures of this resolution; however, the trends are in agreement with the results of molecular modeling studies (see below). Second, there is a large difference in the torsion angles about the C7−C4 bond (Figure 4); in berenil the amidinium group is nearly in the same plane as the phenyl ring (torsion angle 8°), but for furamidine this angle is much larger (24°). The change in torsion angle is associated with the differences in hydrogen bonding; in berenil atom NA interacts with N3 of

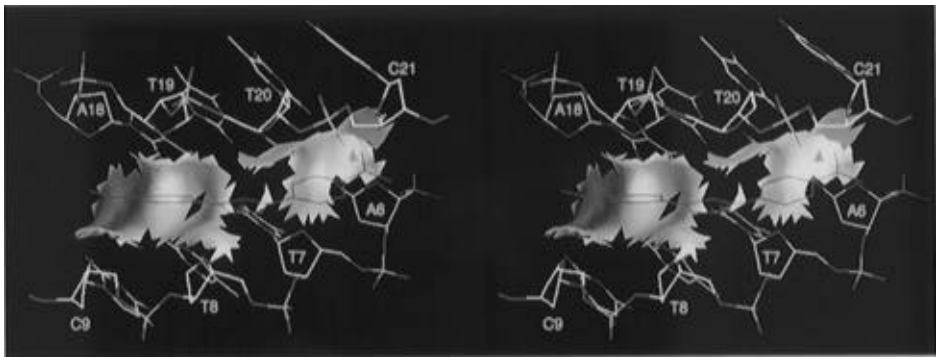

FIGURE 5: Plot of the crystal structure, generated using GRASP (Nicholls et al., 1991), showing the portion of the molecular surface of the DNA within 0.5 Å of the van der Waals surface of furamidine. Two fingers of the surface are visible wrapping round opposite faces of the furan ring, due to close contacts between this ring and the C4′/O4′ edge of the sugar rings of T8 and T20.

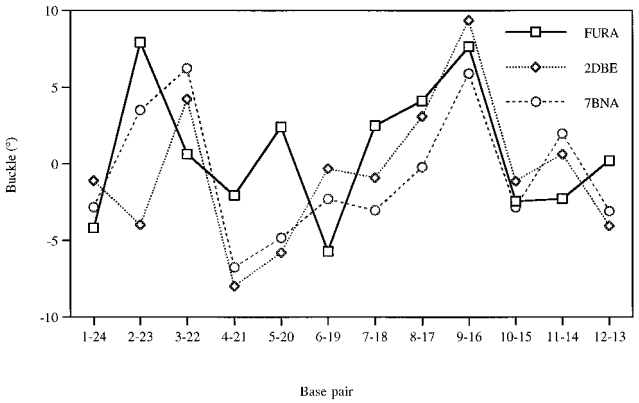

FIGURE 6: Buckle profiles (calculated using the CURVES program) for the furamidine−d(CGCGAATTCGCG)$_2$ (FURA), berenil−d(CGCGAATTCGCG)$_2$ (2DBE), and native (7BNA) crystal structures.

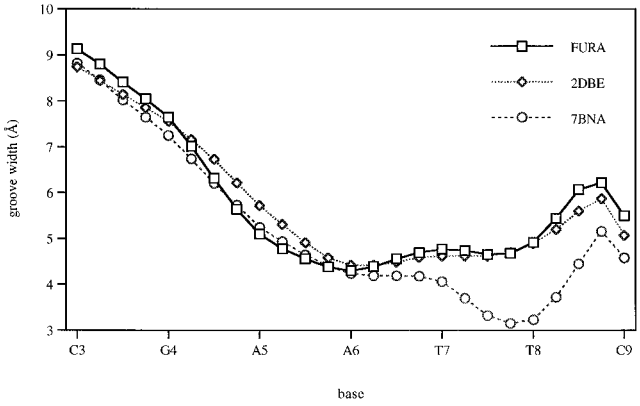

FIGURE 7: Minor groove widths (calculated using CURVES) for the furamidine−d(CGCGAATTCGCG)$_2$ (FURA), berenil−d(CGCGAATTCGCG)$_2$ (2DBE), and native (7BNA) crystal structures.

A18 (3.1 Å), while in the furan complex the equivalent atom, N1, interacts with O2 of T8 (3.1 Å). The shorter effective length of berenil means that, at the other end of the molecule, atom NA′ (equivalent to N1′ in **1**) is too far from O2 of T20 (3.6 Å) for a strong interaction and instead hydrogen-bonds to residues A5 and A6 via a bridging water molecule. It is likely that it is the direct interaction between base pair 5 and the ligand in the present structure, absent in the berenil complex, that is the cause of the observed perturbation in the buckle profile in this region of the DNA. The increased splay angle in furamidine results in its furan linker group lying deeper in the minor groove than the triazene group in berenil, and the increased size of the linker portion may also improve nonbonded interactions with the walls of the minor groove.

Table 1: Ligand−DNA Interaction Energies (Calculated Using AMBER) for the Present Structure and the Analogous Berenil Complex (2DBE)

	berenil complex		furamidine complex	
group	E_{vdW}	E_q	E_{vdW}	E_q
phenylamidinium 1[a]	−15.9	−14.7	−16.4	−16.7
central linker[b]	−3.4	1.6	-6.9	2.0
phenylamidinium 2[c]	−13.2	−14.6	−16.3	−16.2

[a] Unprimed atom labels. [b] Triazene unit in berenil, furan in **1**. [c] Primed atom labels.

Calculation of Interaction Energy Components. In order to provide a more quantitative analysis of the qualitative observations noted above, we have used AMBER to calculate components of the interaction energies between the DNA dodecamer and the drugs in their respective crystal structure conformations. We find that the drug/DNA interaction energy for the complex with furamidine is 10.3 kcal/mol better than for the berenil complex, with 7.1 kcal/mol being due to improved nonbonded interactions and 3.2 kcal/mol due to improved electrostatic interactions. We have examined this in more detail (Table 1) by analyzing the contributions made to these differences by the individual phenylamidinium groups (common to the two drugs) and the central linker moieties. For the first phenylamidinium group, which makes direct contact with the DNA in both structures, the furan structure shows improved electrostatic interactions with the DNA (ΔE_q −2.0 kcal/mol), indicating that the change in the torsion angle of the amidine group between the two structures has a significant effect. For the second phenylamidinium group, which in berenil does not hydrogen-bond directly to the DNA, the differences are, as might be expected, even greater. Furamidine shows improved electrostatic interactions (ΔE_q −1.6 kcal/mol) and improved van der Waals interactions ($\Delta E_{vdW} = -3.1$ kcal/mol). For the central linker region, the calculations show improved nonbonded interactions between the drug and the DNA for furamidine ($\Delta E_{vdW} = -3.5$ kcal/mol). It should be emphasized that such an analysis is necessarily only approximate, as it does not take into account factors such as differences in solvation (particularly relevant to the second amidinium group in the berenil complex) nor does it consider differences in the perturbation energies of the drugs and the DNA.

Semiempirical Calculations on Model Compounds. In order to support the observation regarding the difference in

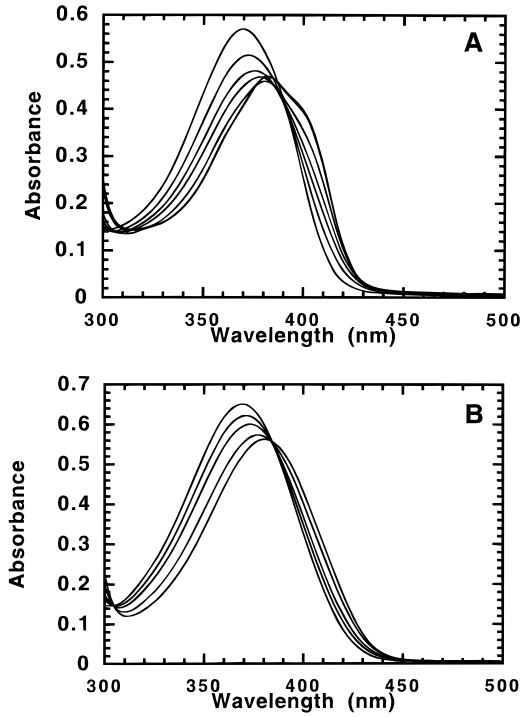

FIGURE 8: Spectrophotometric titrations of furamidine (A) and berenil (B) with d(CGCGAATTCGCG). The titrations were conducted in MES20 buffer at 25 °C. The concentration of the compound in all titrations is 1.7×10^{-5} M. In furamidine−d(CGCGAATTCGCG) spectra the ratios of the compound to $d(CGCGAATTCGCG)_2$ from the top to the bottom are free compound, 10.86, 5.48, 3.67, 2.77, 2.23, 1.86, 1.14, and 0.96. In the berenil−$d(CGCGAATTCGCG)_2$ titrations the ratios of the compound to $d(CGCGAATTCGCG)_2$ from the top to the bottom are free compound, 6, 3, 1.5, and 1.

the splay angles between the phenylamidinium groups in these two structures, we used MOPAC to calculate geometry-optimized structures for the model compounds 1,3-diphenyltriazine and 2,5-diphenylfuran. The MNDO-optimized structure of 1,3-diphenyltriazine shows an angle of 126° between the CA−C4 and CA′−C4′ vectors, while for 2,5-diphenylfuran the angle is 134°. Although the values are both rather larger than we observe crystallographically, the trend is the same; the furan linker produces a larger angle between the two halves of the molecule.

Spectral Characteristics. Absorption spectral results for titrations for furamidine (**1**) with the oligomer $d(CGCGAATTCGCG)_2$ in MES20 buffer are compared in Figure 8A, and similar spectra for berenil are shown in Figure 8B. Addition of the DNA oligomers causes a decrease in extinction coefficient at the maximum wavelength for both compounds. At the concentrations of our experiments berenil has clear isosbestic points in its titration with the oligomer. Furamidine has an isosbestic point at ratios below one, but at ratios above one compound per duplex the isosbestic point is lost (Figure 8A).

Furamidine and berenil have no intrinsic CD bands but have induced CD spectra on complex formation. Addition of furamidine to $d(CGCGAATTCGCG)_2$ results in a positive CD signal at 380 nm, an isoelliptic point at 330 nm, and a negative CD signal at 305 nm (Figure 9). The induced CD signal for berenil is positive throughout the 300−400 nm spectral region (Figure 9).

DNA Affinities. Spectral changes on complex formation were used to construct Scatchard plots (Figure 10) to

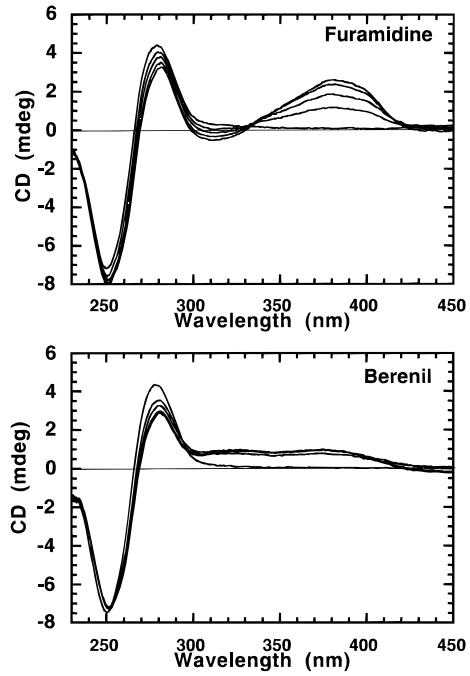

FIGURE 9: CD spectra of furamidine and berenil with d(CGCGAATTCGCG)$_2$. The experiments were conducted in MES10 at 25 °C. In both sets of spectra the ratios of the compound to d(CGCGAATTCGCG) from the top to the bottom at 385 nm are 3, 2, 1, and 0.5.

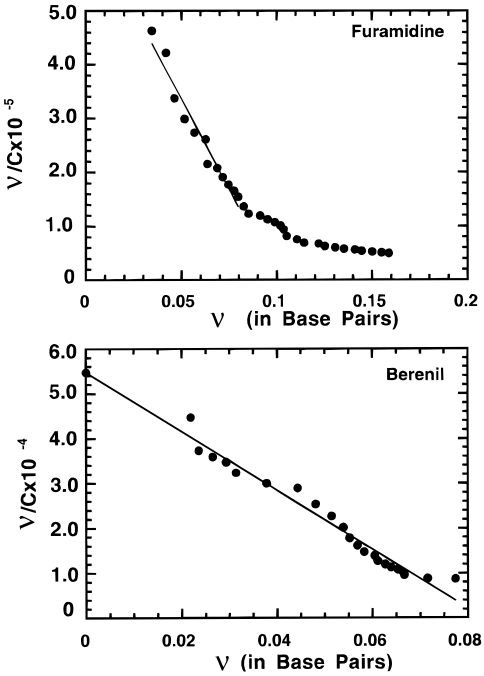

FIGURE 10: Scatchard plots of furamidine and berenil binding to $d(CGCGAATTCGCG)_2$. The experiments were conducted in MES20 at 25 °C. Points in the figure are the data, and the solid lines are the fits using the classical Scatchard equation for independent binding sites. For furamidine $K = 6.7 \times 10^6$ and $n = 1$ per duplex, and for berenil $K = 6.6 \times 10^5$ and $n = 1$ per duplex.

determine the binding constants for furamidine and berenil with $d(CGCGAATTCGCG)_2$. Furamidine binds more strongly to the oligomer than berenil. As can also be seen in the figure, both furamidine and berenil have a strong binding site on the oligomer with a single site per oligomer. Berenil does not show any addition interactions under these conditions, but furamidine also has a set of weaker sites. At

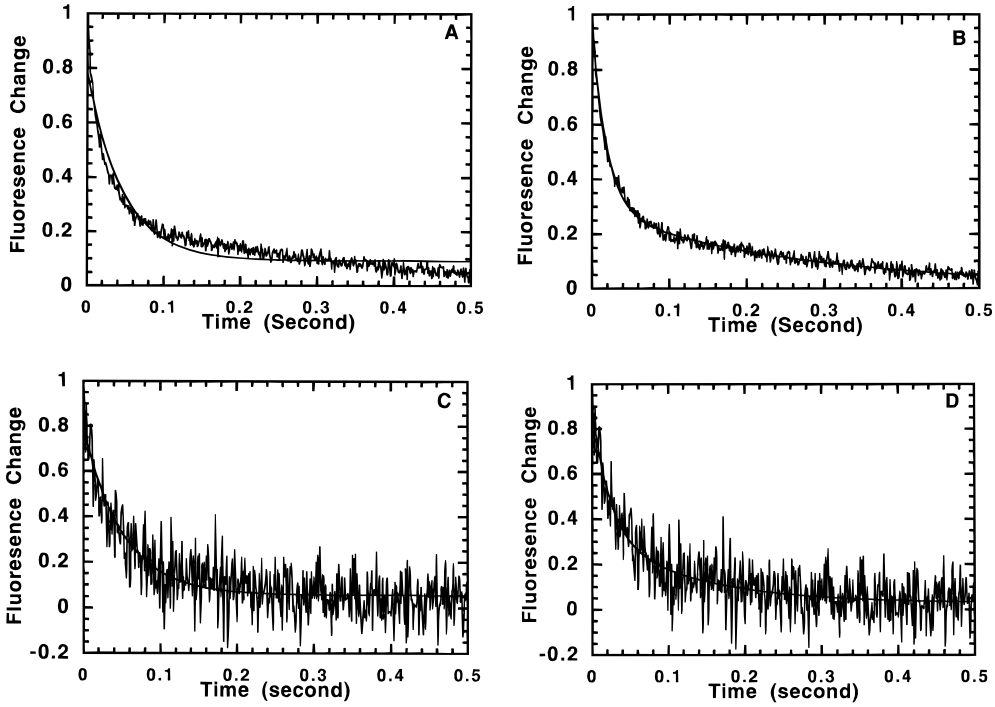

FIGURE 11: Stopped-flow kinetic fluoresence traces for the SDS-driven dissociation of furamidine (A and B) and berenil (C and D) from d(CGCGAATTCGCG)$_2$. The experiments were conducted in MES20 at 20 °C. The ratios of compound to d(CGCGAATTCGCG)$_2$ are 3:1. For furamidine, the smooth line in panel A (k = 21.4 s^{-1}) is the single exponential fit values to the experimental data and in panel B (k_1 = 3.9 s^{-1}, A_1 = 30%, k_2 = 51.5 s^{-1}, and A_2 = 70%) is the dual exponential fit values. For berenil, the smooth line in panel C (k = 27 s^{-1}) is the single exponential fit values to the experimental data and in panel D (k_1 = 44.7 s^{-1}, A_1 = 63%, k_2 =8.1 s^{-1}, and A_2 = 37%) is the dual exponential fit values. The signal to noise is better with furamidine because of its much better fluoresence signal.

low n values, the data were fitted by using the classical Scatchard equation for independent binding sites without cooperativity (Scatchard, 1949):

$$n_s/C = K_s(n - n_s)$$

where C is the free ligand concentration, n is the moles of compound bound per oligomer, n_s is the number of binding sites per oligomer, and K_s is the binding constant.

Complex Dynamics. The spectral changes observed for furamidine and berenil on binding to d(CGCGAATTCGCG)$_2$ can also be used to follow the kinetics of binding. Typical fluorescence versus time stopped-flow kinetic traces for the SDS-driven dissociation of the furamidine and berenil from d(CGCGAATTCGCG)$_2$ are shown in Figure 11. SDS-driven dissociation kinetics results for both compounds can be adequately fitted with single exponential curves at a ratio of one drug per duplex and below (not shown). At higher ratios the results for berenil do not significantly change (Figure 11). The furamidine dissociation has an additional component at higher ratios and requires two exponential curves to fit the data. These results again suggest that the furamidine has a primary strong binding mode to the oligomer and weaker binding modes that are populated at ratios above 1.0 (Figure 11).

DISCUSSION

In spectral titrations with the d(CGCGAATTCGCG)$_2$ sequence, furamidine gives an isosbestic point up to a ratio of one compound per duplex. The isosbestic point is lost as the ratio of furamidine to duplex is increased, and we speculate that binding in the GC terminal regions of the duplex occurs under these conditions. The behavior with berenil is simpler, indicating no significant binding to the GC regions of the oligomer under these conditions. The X-ray results clearly define the minor groove binding mode for furamidine and berenil with d(CGCGAATTCGCG)$_2$. The binding mode of furamidine with GC sites has not yet been characterized crystallographically but has spectral characteristics typical of an intercalation complex (Wilson et al., 1990), though there is evidence from linear dichroism that the short axis of furamidine is inclined to the helix axis, contradicting the classical model of intercalation (Jansen et al., 1993). Breslauer and co-workers (Pilch et al., 1995) have recently shown that at low salt concentrations berenil can intercalate into GC regions of DNA.

Scatchard analysis of the interaction of furamidine with d(CGCGAATTCGCG)$_2$ shows a strong binding site for the minor groove binding mode and a set of much weaker binding sites that represent the GC interactions. Berenil has only a single binding site with the oligomer but has a binding constant that is approximately 10-fold less than the strong binding of furamidine.

The kinetic results also support a single, strong binding mode for both furamidine and berenil at ratios to duplex of 1:1 and below. At higher ratios furamidine shows an additional exponential phase in the dissociation kinetics curves, but berenil does not. The dissociation rate constants are only slightly smaller for furamidine than for berenil, suggesting that furamidine association is significantly faster than for berenil to give the higher observed binding constant differences.

The availability of the crystal structures of both berenil and **1** bound to the same DNA sequence provides a rare opportunity to see if crystallography can provide insight at the molecular level into how the relatively minor difference

in the structure of the ligands can have a marked effect on their DNA-binding affinities. The crystal structures reveal two ways in which the furan linker might promote tighter binding between the ligand and the DNA than the triazene linker. First, by producing a greater splay angle between the phenylamidinium groups, the furan linker increases the effective length of the ligand and improves the registration between the hydrogen bond donor groups of the ligand and acceptor groups on the DNA bases. Second, the more bulky and hydrophobic furan linker has more extensive van der Waals interactions with the walls of the minor groove than the triazene linker in berenil. The two atoms, CB and CB′ of the furan ring are ideally placed to form close nonbonded contacts with the backbone atoms from each strand of the DNA, which form the outer-edge surface of the minor groove (Neidle, 1992), and such close distances are observed in this crystal structure. We also suggest that the slightly longer length of furamidine compared to berenil enables two direct drug−DNA hydrogen bond interactions to take place, as compared to the one for berenil. The water-mediated berenil contact is likely to be somewhat weaker than these.

A considerable number of minor groove drug−DNA complex structures have now been solved by X-ray crystallography. Some general features are now apparent from these structures: (i) the narrow cross-section of the ligand molecules complements the narrow minor groove of AT regions of DNA; (ii) drug stabilization in the binding site is achieved by numerous nonbonded contacts, especially with the hydrophobic atoms populating the upper edges of the minor groove; (iii) conservative changes in ligand structure, as exemplified in the present study, do not result in significant changes in DNA geometry. We have shown here that macroscopic measurements of changes in DNA-binding affinity between berenil and furamidine can be rationalized at the molecular level by both molecular modeling and X-ray crystallography in terms of these features. This in turn suggests that further rational design of new minor groove binding ligands can now be undertaken with confidence when, as in the case of furamidine and related compounds, the goal is enhanced affinity to AT-rich DNA sequences as this correlates well with efficacy against *P. carinii* and other microbial infections (Boykin et al., 1995).

REFERENCES

Boykin, D. W., Kumar, A., Spychala, J., Zhou, M., Lombardy, R. J., Wilson, W. D., Dykstra, C. C., Jones, S. K., Hall, J. E., Tidwell, R. R., Laughton, C. A., Nunn, C. M., & Neidle, S. (1995) *J. Med. Chem. 38*, 912−916.

Brown, D. G., Sanderson, M. R., Skelly, J. V., Jenkins, T. C., Brown, T., Garman, E., Stuart, D. I., & Neidle, S. (1990) *EMBO J. 9*, 1329−1334.

Brown, D. G., Sanderson, M. R., Garman, E., & Neidle, S. (1992) *J. Mol. Biol. 226*, 481−490.

Brunger, A. T., Kuriyan, J., & Karplus, M. (1987) *Science 235*, 458−460.

Coll, M., Aymami, J., van der Marel, G., van Boom, J., Rich, A., & Wang, A. H. J. (1989) *Biochemistry 28*, 310−320.

Das, B. P., & Boykin, D. W. (1977) *J. Med. Chem. 20*, 531−536.

Fasman, G. D. (1975) *Nucleic Acids: Hand Book of Biochemistry and Molecular Biology*, p 589, CRC Press, Cleveland, OH.

Fede, A., Labhardt, A., Bannwarth, W., & Leupin, W. (1991) *Biochemistry 30*, 11377−11388.

Gao, Y. G., Sriram, M., Denny, W. A., & Wang, A. H. J. (1993) *Biochemistry 32*, 9639−9648.

Goodsell, D., & Dickerson, R. E. (1986) *J. Med. Chem. 29*, 727−33.

Goodsell, D. S., Kopka, M. L., & Dickerson, R. E. (1995) *Biochemistry 34*, 4983−4993.

Holbrook, S. R., Dickerson, R. E., & Kim, S.-H. (1985) *Acta Crystallogr. B41*, 255−262.

Jansen, K., Lincoln, P., & Nordén, B. (1993) *Biochemistry 32*, 6605−6612.

Jenkins, T. C., Lane, A. N., Neidle, S., & Brown, D. G. (1993) *Eur. J. Biochem. 213*, 1175−1184.

Jones, T. A., Zhou, J.-Y., Cowan, S. W., & Kjeldgaard, M. (1991) *Acta Crystallogr. A47*, 110−119.

Kibler-Herzog, L., Kell, B., Zon, G., Shinozuka, K., Mizan, S., & Wilson, W. D. (1990) *Nucleic Acids Res. 18*, 3545−3555.

Klevit, R. E., Wemmer, D. E., & Reid, B. R. (1986) *Biochemistry 25*, 3296−3303.

Kopka, M. L., Yoon, C., Goodsell, D., Pjura, P., & Dickerson, R. E. (1985) *J. Mol. Biol. 183*, 553−563.

Kumar, S., Jaseja, M., Zimmermann, J., Yadagiri, B., Pon, R. T., Sapse, A. M., & Lown, J. W. (1990) *J. Biomol. Struct. Dyn. 8*, 99−121.

Kumar, S., Bathini, Y., Joseph, T., Pon, R. T., & Lown, J. W. (1991) *J. Biomol. Struct. Dyn. 9*, 1−21.

Laughton, C. A., Jenkins, T. C., Fox, K. R., & Neidle, S. (1990) *Nucleic Acids Res. 18*, 4479−4488.

Lavery, R., & Sklenar, H. (1988) *J. Biomol. Struct. Dyn. 6*, 63−91.

Lee, M., Chang, D. K., Hartley, J. A., Pon, R. T., Krowicki, K., & Lown, J. W. (1988) *Biochemistry 27*, 445−455.

Neidle, S. (1992) *FEBS Lett. 298*, 97−99.

Nicholls, A., Sharp, K. A., & Honig, B. (1991) *Proteins 11*, 281−296.

Orozco, M., Laughton, C. A., Herzyk, P., & Neidle, S. (1990) *J. Biomol. Struct. Dyn. 8*, 359−373.

Parkinson, J. A., Barber, J., Douglas, K. T., Rosamond, J., & Sharples, D. (1990) *Biochemistry 29*, 10181−10190.

Patel, D. J., & Shapiro, L. (1986) *J. Biol. Chem. 261*, 1230−1240.

Pearlman, D. A., Case, D. A., Caldwell, J. C., Seibel, G. L., Chandra Singh, U., Weiner, P., & Kollman, P. A. (1991) *AMBER 4.0*, University of California, San Francisco.

Pelton, J. G., & Wemmer, D. E. (1989) *Proc. Natl. Acad. Sci. U.S.A. 86*, 5723−5727.

Pilch, D. S., Kirolos, M. A., Liu, X. Plum, G. E., & Breslauer, K. J. (1995) *Biochemistry 34*, 9962−9976.

Scatchard, G. (1949) *Ann. N.Y. Acad. Sci. 51*, 660−672.

Searle, M. S., & Embrey, K. J. (1990) *Nucleic Acids Res. 18*, 3753−3762.

Singh, M. P., Kumar, S., Joseph, T., Pon, R. T., & Lown, J. W. (1992) *Biochemistry 31*, 6453−6461.

Stewart, J. P. P. (1990) *Mopac 6.0 (QCPE)*, available from the Quantum Chemistry Program Exchange, Indiana University, Bloomington, IN 47405.

Tabernero, L., Verdaguer, N., Coll, M., Fita, I., van der Marel, G. A., van Boom, J. H., Rich, A., & Aymami, J. (1993) *Biochemistry 32*, 8403−8410.

Tanious, F. A., Jenkins, T. C., Neidle, S., & Wilson, W. D. (1992) *Biochemistry 31*, 11632−11640.

Ulyanov, N. B., & Zhurkin, V. B. (1984) *J. Biomol. Struct. Dyn. 2*, 361−385.

Weiner, S. J., Kollman, P. A., Nguyen, D. T., & Case, D. A. (1986) *J. Comput. Chem. 7*, 230−252.

Wilson, W. D., Wang, Y. H., Krishnamoorthy, C. R., & Smith, J. C. (1985) *Biochemistry 24*, 3991−3999.

Wilson, W. D., Tanious, F. A., Buczak, H., Venkatramanan, M. K., Das, B. P., & Boykin, D. W. (1990) in *Molecular Basis of Specificity in Nucleic Acid−Drug Interactions: Jerusalem Symposia on Quantum Chemistry and Biochemistry* (Pullman, B., & Jortner, J., Eds.) Vol. 23, pp 331−353, Kluwer Academic Publishers, Dordrecht, The Netherlands.

Zakrzewska, K., Lavery, R., & Pullman, B. (1987) *J. Biomol. Struct. Dyn. 4*, 833−843.

Zhurkin, V. B., Ulyanov, N. B., Gorin, A. A., & Jernigan, R. L. (1991) *Proc. Natl. Acad. Sci. U.S.A. 88*, 7046−7050.

BI952162R